CHROMOSPHERIC AND CORONAL HEATING MECHANISMS

P. ULMSCHNEIDER
Institut für Theoretische Astrophysik, Universität Heidelberg,
Tiergartenstr. 15, D--69121 Heidelberg, Germany

1. Introduction

The present work discusses the basic physical mechanisms which produce the heating of stellar chromospheres and coronae. As extensive reviews on this subject have been published elsewhere (Narain & Ulmschneider [2], (Paper I), Narain & Ulmschneider [3] (Paper II) as well as Ulmschneider [4] (Paper III)) the present paper concentrates on the physics of the heating processes. For additional literature as well as for additional reviews see Papers I to III. Section 2 discusses the necessity of chromospheric and coronal heating and describes the elementary heating processes. Section 3 outlines the hydrodynamic heating mechanisms and Section 4 the magnetic heating mechanisms.

2. Necessity of Mechanical Heating of Chromospheres and Coronae

Consider a gas element in the chromosphere. The amount of heat dQ *(erg /cm^3)* flowing across its boundaries raises the entropy in the element by $dS = dQ / \rho T$, where ρ is the density and T the temperature. For a plane parallel atmosphere one can write the entropy conservation law

$$\rho T\left(\frac{\partial S}{\partial t}+\frac{\partial S}{\partial z}\right)=\Phi_R+\Phi_C+\Phi_V+\Phi_J+\Phi_M \qquad (1)$$

Here z is height, t time, v the gas velocity and Φ heating rates (*erg/ cm^3 s*). Eq. (1) states that the entropy in the gas element increases if from the outside, energy is supplied by radiative, thermal conductive, viscous, Joule and mechanical heating. Mechanical heating comprises all processes which convert nonradiative, nonconductive hydrodynamic or magnetic energy (henceforth called mechanical energy) flowing through the element into microscopic random thermal motion.

As the chromosphere exists on the Sun for billions of years one can neglect the term $\partial S / \partial t$ in Eq. (1) in a time-averaged model. With a solar wind mass loss

Z. Mouradian and M. Stavinschi (eds.),
Theoretical and Observational Problems Related to Solar Eclipses, 95-102.

rate of $\dot{M} = 10^{-14}\, M_\odot/y$ one can compute a wind speed $v = \dot{M}/(4\pi\rho R^2_\odot) \approx 1.1\ 10^{-11}/\rho$, from which one finds very low flow speeds. Even in the transition layer e.g. with $\rho = 2.3\ 10^{-15}$g/cm^3 and T=4.5 10^5 K one has a flow speed of only v=4.7 10^3 compared to a sound speed of c_S=1 10^7 cm/s. Thus the entire LHS of Eq. (1) can be neglected. Below we will show that in the chromosphere Φ_C, Φ_V and Φ_J can also be neglected, while Φ_C is important in the transition layer and corona. Using a gray expression for the radiative heating rate we thus find for the chromosphere

$$4\pi\kappa\left(\bar{J} - B\right) + \Phi_M = 0 \qquad (2)$$

Here $\bar{\kappa}$ is the Rosseland opacity, $\bar{J}$ the frequency integrated mean intensity, $B = \sigma T^4/\pi$ the frequency integrated Planck function and σ the Stefan-Boltzmann constant. In the special case of *radiative equilibrium* one has $\Phi_M = 0$ and finds $\bar{J} = B$. On the stellar surface one has $\bar{J} = \sigma T_{eff}^4 / 2\pi$, where T_{eff} is the effective temperature and the factor 1/2, as there is intensity only away from the star. In radiative equilibrium one therefore finds $T = 1/2^{1/4}\ T_{eff} \approx 0.8\ T_{eff}$, that is, in absence of mechanical heating the outer stellar regions would have temperatures of the order of the boundary temperature. However, as a chromosphere is a layer where the temperature rises in outward direction to values $T >> T_{eff}$, it is clear that $B >> \bar{J}$ and therefore one must have $\Phi_M >> 0$. This shows that for chromospheres mechanical heating is essential. In addition, as the energy loss of the transition layer and corona cannot be balanced by thermal conduction from a reservoir at infinity, but must ultimately be supplied from the stellar interior, we conclude that for transition layers and coronae, mechanical heating is also essential.

Moreover, chromospheres and coronae can only be maintained if mechanical heating is constantly applied. The time scale, in which an excess temperature will cool down to the boundary temperature, if the mechanical heating were suddenly disrupted, is given by the *radiative relaxation time*

$$t_{Rad} = \frac{\Delta E}{\Phi_R} = \frac{\rho c_v \Delta T}{16\bar{\kappa}T^3\Delta T} = \frac{\rho c_v}{16\bar{\kappa}\sigma T^3} \approx 1.1 \cdot 10^3\, s \qquad (3)$$

Here from a typical solar model at z = 1280 km: T= 6200 K, p = 4.4 dyn/cm^2, $\bar{\kappa}/\rho$ = 4.1 10^{-4} cm^2/g, c_v = 9.6 10^7 erg/gK, σ =5.6 10^{-5} $erg/cm^2\ s\ K^4$. It is seen that in timescales of a fraction of an hour the chromosphere would cool down to the boundary temperature if mechanical heating would suddenly be interrupted.

Table1 summarizes the mechanisms which are thought to provide a steady supply of mechanical energy to balance the chromospheric and coronal losses. Here occasional transient and localized heating events like large flares are not considered because they do not contribute appreciably to the persistent chromospheric and coronal

heating. The term heating mechanism comprises three physical aspects, the *generation* of a carrier of mechanical energy, the *transport* of mechanical energy into the chromosphere and corona and the *dissipation* of this energy in these layers. Table.1 shows the various proposed energy carriers which can be classified into two main categories as *hydrodynamic* and *magnetic* mechanisms. The magnetic mechanisms can be subdivided further into wave- or AC-mechanisms and current sheet- or DC-mechanisms. Also in Table.1 the mode of dissipation of these mechanical energy carriers is indicated. Ultimately these mechanical energy carriers derive their energy

TABLE 1 Mechanical heating mechanisms for stellar chromospheres and coronae, P is the wave period and P_A the acoustic cut-off period.

energy carrier	dissipation mechanism
hydrodynamic heating mechanisms	
acoustic waves, $P < P_A$	shock dissipation
pulsational waves, $P > P_A$	shock dissipation
magnetic heating mechanisms	
1. alternating current (AC) or wave mechanisms	
slow mode mhd waves, longitudinal mhd tube waves	shock dissipation
fast mode mhd waves	Landau damping
Alfvén waves (transverse, torsional)	resonance heating compressional viscous heating turbulent heating Landau damping
magnetoacoustic surface waves	mode-coupling phase-mixing resonant absorption
2. direct current (DC) mechanisms	
current sheets	reconnection (turbulent heating, wave heating)

from the nuclear processes in the stellar core from where the energy is transported in he form of radiation and convection to the stellar surface. In late-type stars the mechanical energy generation arises from the gas motions of the surface convection zones. These gas motions are largest in the regions of smallest density near the top boundary of the convection zone. Due to this the mechanical energy carriers, particularly the waves, are generated in a narrow surface layer.

Let us now discuss the *elementary heating processes*. In the dissipation process, mechanical energy is converted into heat. That is, organized motion or potential energy is converted into random thermal motion. As will be shown below, an

efficient conversion process is almost always associated with the generation of large variations of the physical variables over very small scales. For instance, it has been known for a long time that an efficient way to dissipate acoustic waves is the formation of shocks, where the physical variables abruptly vary over distances of a molecular mean free path.

Consider a typical acoustic or magnetohydrodynamic disturbance in the solar chromosphere with characteristic parameters, size $\Delta L=200$ *km*, temperature $\Delta T=1000K$, velocity $\Delta v=3$ *km/s* and magnetic field perturbation $\Delta B=10$ *G*. Using appropriate values for the thermal conductivity $\kappa_{\tau\eta} = 10^5$ *erg/cm s K*, viscosity $\eta_{vis} = 5\ 10^{-4}$ *dyn s/cm²* and electrical conductivity $\lambda_{el} = 2\ 10^{10}$ *s*$^{-1}$ we find for the *thermal conductive heating rate*

$$\Phi_C = \frac{d}{dz}\kappa_{th}\frac{dT}{dz} \approx \frac{\kappa_{th}\Delta T}{\Delta L^2} \approx 3\cdot 10^{-7} \quad \left[\frac{erg}{cm^3 s}\right] \tag{4}$$

the *viscous heating rate*

$$\Phi_V = \eta_{vis}\left(\frac{dv}{dz}\right)^2 \approx \frac{\eta_{vis}\Delta v^2}{\Delta L^2} \approx 1\cdot 10^{-7} \quad \left[\frac{erg}{cm^3 s}\right] \tag{5}$$

the *Joule heating rate*:

$$\Phi_J = \frac{J^2}{\lambda_{ei}} = \frac{c_L^2}{16\pi^2\lambda_{el}}(\nabla\times B)^2 \approx \frac{c_L^2\Delta B^2}{16\pi^2\lambda_{el}\Delta L^2} \approx 7\cdot 10^{-5} \left[\frac{erg}{cm^3 s}\right] \tag{6}$$

Here J is the current density and c_L the light velocity. The three heating rates show that normally these processes are inadequate to balance the empirical chromospheric cooling rate of $-\Phi_R = 10^{-1}$ erg/ cm ^{3} s. Only when the length scale ΔL is considerably decreased, can the heating rates be raised to acceptable levels. For acoustic waves as well as slow mode mhd- and longitudinal mhd tube waves, this is accomplished by shock formation. For magnetic cases, by the formation of current sheets.

3. Hydrodynamic Heating Mechanisms

There are two hydrodynamic mechanisms *acoustic waves* and *pulsational waves*. Acoustic waves have periods less then the acoustic cut-off period $P_A = 4\pi\ c_S / (\gamma g)$ while pulsational waves have periods $P>P_A$ (see Papers I and II for details). Acoustic waves are generated in the surface convection zones of late-type stars and by radiative instabilities in early-type stars, they heat by shock dissipation. Pulsational waves, most prominent in Mira-star pulsations, but also in other late-type giants, are generated by

the *kappa-mechanism* and related processes. Like acoustic waves, pulsational waves heat by shock dissipation.

4. Magnetic Heating Mechanisms

4.1. MODE-COUPLING

This mechanism is not a heating process by itself, but converts wave modes, which are difficult to dissipate, by non-linear coupling into other modes, where the dissipation is more readily achieved. Typical cases are the conversion of transverse or torsional Alfvén waves into acoustic-like longitudinal tube waves. For examples of these two processes see Papers I and II.

4.2. RESONANCE HEATING

Resonance heating occurs, when upon reflection of Alfvén waves at the two foot points of the coronal loops, one has constructive interference. For a given loop length $l_{||}$ and Alfvén speed c_A, resonance occurs, when the wave period is $mP = 2\ l_{||}\ c_A$, , m being a positive integer. Waves which fulfill the resonance condition are trapped and after many reflections are dissipated by Joule-; thermal conductive or viscous heating. Examples of this process are given in Papers I and II.

4.3. COMPRESSIONAL VISCOUS HEATING

Compressional viscous heating, recently proposed by Strauss [7] (see also Paper II), is a very promising mechanism for coronal regions, where the gyro frequency is much larger than the collision frequency. Swaying an axial magnetic flux tube sideways with velocity $\mathbf{v}$ results in a transverse Alfvén wave which is incompressible $\nabla\cdot\mathbf{v}=0$ to first order. This is different for tubes with helicity, where one has $\nabla\cdot\mathbf{v}\approx\rho/\rho$. With an increase of the density, the magnetic field is compressed and the gyro frequency increased. Gyrating around the field lines more quickly, the ions after colliding with each other, generate larger velocities in non-perpendicular directions as well, which constitutes the heating process.

4.4. TURBULENT HEATING

In a turbulent flow field with high Reynolds number there are bubbles of all sizes. The energy usually is put into the largest bubbles. Because of the large inertial forces the big bubbles are ripped apart into smaller bubbles, and these in turn into still smaller ones etc. This process is called turbulent cascade. A turbulent flow field can be described by three characteristic quantities, density ρ_0, bubble scale $l_k = 2\pi/k$, and the mean velocity u_k of such bubbles. k is the wavenumber. It is easily seen, that from these three quantities only one combination for a heating rate can be formed:

$$\Phi_k = \rho_0 \frac{u_k^3}{l_k} \quad \left[\frac{erg}{cm^3 s}\right] \tag{7}$$

If there are no other losses, like by radiation, all the energy which is put in at the largest bubbles must reappear in the smaller bubbles etc. Thus if *k1, k2, ...* represents a series of smaller and smaller bubbles one must have $\Phi_{k1} = \Phi_{k2} = ... =$ const. This implies

$$u_k \sim l_k^{1/3} \tag{8}$$

which is the *Kolmogorov law*. The range $l_{k1}...l_{k2}$ of validity of this law is called the *inertial range*. Consider what happens if l_k becomes very small. From Eqs. (8) and (11) one finds for the viscous heating rate $\Phi_V = \eta_{vis}(du/dl)^2 \approx \eta_{vis} u_k^2 / l_k^2 \approx \eta_{vis} l_k^{-4/3}$ which goes to infinity for $l_k \rightarrow 0$. Thus at some small enough scale, viscous heating sets in and the inertial range ends. It is seen that turbulent heating lives from the formation of small scales. One can visualize the process as follows. Because of the continuous splitting of bubbles into smaller sizes, with the velocities decreasing much less rapidly, one eventually has close encounters of very small bubbles with large velocity differences where viscous heating dominates. In magnetic flux tubes the turbulent cascade is supposed to happen in transverse direction to the field (see Papers I and II).

4.5. LANDAU DAMPING

Landau damping occurs at coronal heights, where the collision rate becomes small. As Chen ([1] Fig. 7.17) has well explained, this process is analogous to surfing on ocean waves. When surfing, a surfboard rider launches himself in propagation direction into the steepening part of an incoming wave and gets further accelerated by this wave. In Landau damping, the propagating wave accelerates gas particles which, due to their particle distribution function, happen to have similar direction and speed as the wave. Because a distribution function normally has many more slower particles than faster ones, the wave looses energy to accelerate the slower particles. This gained energy is then shared with other particles in the process to reestablish the distribution function which constitutes the heating mechanism.

4.6. RESONANT ABSORPTION

In the process of resonant absorption one considers magnetoacoustic surface waves in a magnetic field B which points in z-direction, and varies from B_1 to B_2 in x-direction (see Figure 1). The surface wave, with its field perturbation $\delta B = B'_x$ in x-direction, has a phase speed $v_{ph} = ((B_1^2 + B_2^2)/(4\pi(\rho_1 + \rho_2))^{1/2}$, such that at an intermediate position x_0, the phase speed becomes equal to the local Alfvén speed

$c_{Ao} = B(x_0)/\sqrt{4\pi\rho(x_0)}$. In panel a of Figure -1 consider the wave fronts of the peak (drawn) and trough (dotted) of a surface wave. Because to the right of x_0, the Alfvén speed is larger and to the left smaller, the wave fronts at a later time get tilted, relative to the phase, propagating with speed c_{Ao} (see panel b). At a still later time (panel b) the wave fronts get tilted even further and approach each other closely at the position x_0. This leads to small scales and intense heating at that field line. For the recent extensive analytical and numerical work on this heating process see Papers I and II as well as the references therein.

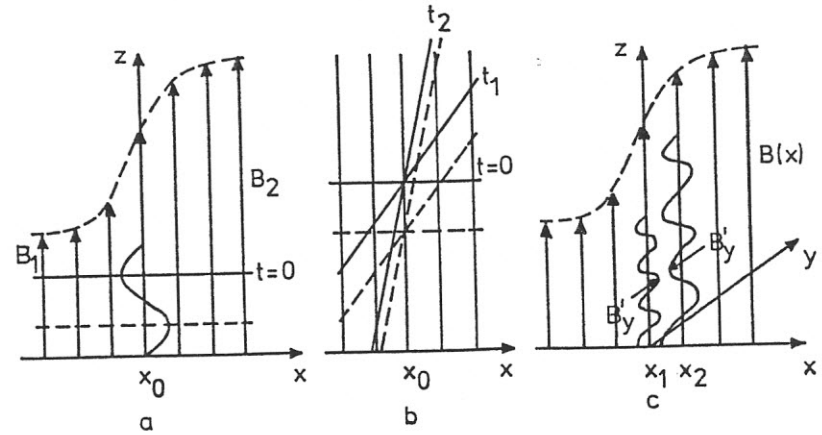

Figure 1 In a field pointing in z-direction, where the field strength varies in x-direction: a) resonant absorption of a surface wave (shaking in x-direction), wave fronts at time t=0, b) these wave fronts at subsequently later times t_1, and t_2, c) phase-mixingof a surface wave (shaking in y-direction).

4.7. PHASE-MIXING

For phase-mixing (c.f. panel c of Figure 1) one considers the same magnetic field geometry as in panel a of Figure 1, however, the field perturbation $\delta B = B'_x$ of the wave is now in y-direction, perpendicular to the x- and z-directions. As the Alfén speeds of two closely adjacent regions x_1 and x_2 in x-direction are different, it is seen that after propagating some distance Δz, the fields $B'_y(x_1)$ and $B'_y(x_2)$ will be very different, leading to a current sheet and strong dissipation. Here again it is the appearance of small scale structures which lead to dissipation (see Papers I and II).

4.8. RECONNECTION

As examples of the DC heating mechanisms I discuss two situations where current sheets are thought to exist [6], shows an arcade system, which by slow motion is

laterally compressed and develops a current sheet, where oppositely directed fields reconnect. The other example by Parker [5] pictures a tangled and braided web of coronal loops created by slow foot point motions. As the motions put in more and more energy, the system tries to return to its minimum energy configuration. This can only be done by reconnection. At many locations in the web, oppositely directed fields occur giving rise to local current sheets, which by reconnection (in the form of microflares) release the magnetic field energy. The energy is dissipated both directly and via the generation of waves and turbulence. Note that reconnection likewise happens in small scale regions.

References

1. Chen, F.F. (1984), *Introduction to Plasma Physics and Controlled Fusion* 2^{ed}, Vol 1, Plasma Physics,Plenum Press, New York
2. Narain, U., Ulmschneider, P. (1990), *Space Sci. Rev.* **54**, 377 (Paper I)
3. Narain, U., Ulmschneider, P.); (1996), *Space Sci. Rev.* **75**, 453 (Paper II)
4. Ulmschneider, P. (1996), in: *Cool Stars Stellar Systems and the Sun*, ASP Conf. Ser., R. Pallavicini, A.K. Dupree (eds.) in press (Paper III)
5. Parker, E.N. (1992), *J. Geophys. Res.* **97**, 4311
6. Priest, E.R. (1991), in *Mechanisms of Chromospheric and Coronal Heating*, Ulmschneider P., Priest E.R., Rosner R., (eds.) Springer, Berlin, p 520
7. Strauss, H.R. (1991), *Geophys. Res. Let.* **18**, 77

RECONSTRUCTION OF THE LARGE-SCALE DISTRIBUTION OF CORONAL ELECTRONS FROM ECLIPSE DATA

F. CLETTE
Observatoire Royal de Belgique,
Brussels, Belgium

Abstract. Mathematical models of the global electron density distribution in the corona were first constructed from solar eclipse images at the end of the last century. Since then, the complexity of these density models has increased steadily, as additional free parameters and new mathematical tools were incorporated. The ultimate goal of this effort has always been to improve the representation of the inhomogeneous coronal structure, while maintaining a restricted set of parameters. This review puts the successive steps of this maturation process in a general perspective. A recent model, developed at the Royal Observatory of Belgium for the 1991 and 1994 eclipses, is described to illustrate the modeling techniques and some current issues.

1. Introduction

The analysis of global properties of the solar corona, using polarized white-light observations made during solar eclipses, began about one hundred years ago. Since the true nature of the diffusing particles, i.e. the free electrons, was discovered, much progress has been achieved in our understanding the overall density distribution of the coronal plasma and of its time evolution. This long-term effort is justified by the multiple repercussions of large-scale models of the coronal electron density in the field of solar physics. These models help in the interpretation of coronal observations at radio and X-ultraviolet wavelengths, and they also provide constraints on the plasma density, temperature and velocity [1, 2, 3]. Furthermore, these global distributions are representative of the concept of the so-called "background corona" [4] and constitute the first step in the determination of the F corona distribution.

During the last decade, the availability of new computing tools brought a new impulse to this kind of research, and new models were recently introduced with a degree of complexity that allows a more detailed and more realistic representation of the inhomogeneous coronal medium. This evolution will be briefly retraced here.

2. Fundamental Integral Equations and the "Power Law" Family of Solutions

The tangential and radial components of the observed K corona intensity, K_t and K_r, are given by the following integral equations:

Z. Mouradian and M. Stavinschi (eds.),
Theoretical and Observational Problems Related to Solar Eclipses, 103-109.